iScience

CellPress
OPEN ACCESS

Article

# A plant receptor domain with functional analogies to animal malectin disables ER stress responses upon infection

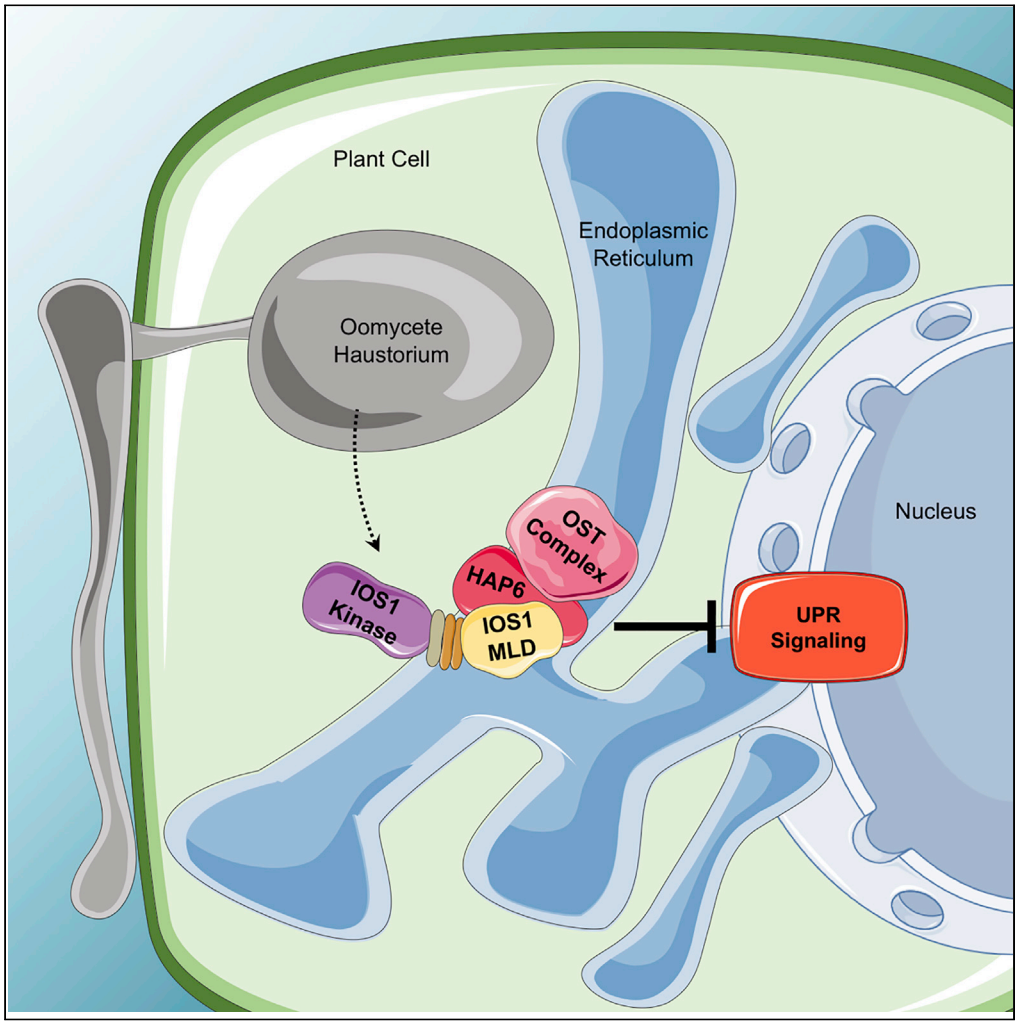


Laïla Giordano, Valérie Allasia, Alexandra Cremades, Sophie Hok, Franck Panabières, Béatrice Bailly-Maître, Harald Keller

harald.keller@inrae.fr

## Highlights

The Unfolded Protein Response (UPR) in plants impairs downy mildew infection

The pathogen exploits a molecular mechanism of the host cell to promote disease

The extracellular domain of the receptor IOS1 attenuates the pathogen-induced UPR

IOS1 interacts with the ribophorin HAP6 in the ER to fine-tune the UPR

Giordano et al., iScience 25, 103877
March 18, 2022 
https://doi.org/10.1016/j.isci.2022.103877

iScience

CellPress
OPEN ACCESS

Article

# A plant receptor domain with functional analogies to animal malectin disables ER stress responses upon infection

Laïla Giordano,[1] Valérie Allasia,[1] Alexandra Cremades,[1] Sophie Hok,[1] Franck Panabières,[1] Béatrice Bailly-Maître,[2] and Harald Keller[1,3,*]

## SUMMARY

**Malectins from the oligosaccharyltransferase (OST) complex in the endoplasmic reticulum (ER) of animal cells are involved in ER quality control and contribute to the Unfolded Protein Response (UPR). Malectins are not found in plant cells, but malectin-like domains (MLDs) are constituents of many membrane-bound receptors. In *Arabidopsis thaliana*, the MLD-containing receptor IOS1 promotes successful infection by filamentous plant pathogens. We show that the MLD of its exodomain retains IOS1 in the ER of plant cells and attenuates the infection-induced UPR. Expression of the MLD in the *ios1-1* knockout background is sufficient to complement infection-related phenotypes of the mutant, such as increased UPR and reduced disease susceptibility. IOS1 interacts with the ER membrane-associated ribophorin HAP6 from the OST complex, and *hap6* mutants show decreased pathogen-responsive UPR and increased disease susceptibility. Altogether, this study revealed a previously uncharacterized role of a plant receptor domain in the regulation of ER stress during infection.**

## INTRODUCTION

In eukaryotes, stress situations that generate unfolded or misfolded proteins or excessive protein synthesis trigger the unfolded protein response (UPR) in the endoplasmic reticulum (ER). The UPR aims at restoring cellular homeostasis by arresting protein synthesis, and by repairing or degrading misfolded proteins. If recovery of homeostasis is impossible, the UPR engages programmed cell death (Hetz, 2012; Hiramatsu et al., 2015; Hetz et al., 2020). In plants, infection with microbial pathogens frequently results in the onset of the UPR, which can in turn contribute to immune responses (Xu et al., 2019; Chakraborty et al., 2020) and programmed cell death, responses that aim at confining microbes and limiting the spreading of disease (Carvalho et al., 2014; Mishiba et al., 2013; Verchot and Pajerowska-Mukhtar, 2021). To countervail such responses, oomycete pathogens from the genus *Phytophthora* attenuate the UPR by secreting effectors into host cells that interact with ER stress-regulatory proteins (Jing et al., 2016; Fan et al., 2018; Qiang et al., 2021). However, the molecular mechanisms that connect biotic stress to the UPR and the plant immune system remain largely unknown. The UPR signaling network involves two pathways in plants, which are similar to those found in animal cells. One is mediated by inositol-requiring protein 1 (IRE1) and the transcription factor (TF) bZIP60. The other involves the TFs bZIP28 and bZIP17, which are functional homologs of activating transcription factor 6 (ATF6) in animal cells (Nawkar et al., 2018). The third animal UPR signaling pathway, which is mediated by the protein kinase RNA (PKR)-like ER kinase (PERK), has not yet been uncovered in plants. To avoid that unrestrained UPR leads to cell and tissue damage, eukaryotes possess regulatory mechanisms to tightly control the response (Angelos et al., 2017).

In animal cells, malectins control the glycosylation status of proteins (Schallus et al., 2008; Galli et al., 2011). Under ER stress conditions, malectin synthesis is induced and the protein interacts at the ER membrane with the ribophorins I and II (RPN1 and RPN2) to assure retention of misfolded proteins and to perform quality control on such proteins after the addition of N-glycosylations (Chen et al., 2011; Qin et al., 2012). RPN1 and RPN2 are subunits of the OST complex, which transfers oligosaccharides to nascent proteins in the ER. In Arabidopsis, three genes encode ribophorins. Two of the encoded proteins have similarities with RPN1 (OST1A, AT2G01720 and OST1B, AT1G76400), whereas the third (HAP6, AT4G21150) appears to be an RPN2 ortholog. These ribophorins are part of the essential core of the OST complex in

[1]Université Côte d'Azur, INRAE, CNRS, UMR1355-7254, ISA, 06903 Sophia Antipolis, France

[2]Université Côte d'Azur, INSERM, U1065, C3M, 06200 Nice, France

[3]Lead contact

*Correspondence: harald.keller@inrae.fr

https://doi.org/10.1016/j.isci.2022.103877

Arabidopsis (Jeong et al., 2018). However, little is known about the role of the RPN-like proteins in Arabidopsis, and functional data are only available for the RPN2 ortholog HAP6, which has been characterized in a genetic screen for haploid-disrupting (hapless) mutations that lead to failure in pollen grain development, pollen tube growth, and guidance in the ovary (Johnson et al., 2004).

Despite the apparent conservation of proteins from the OST complex among animals and plants, counterparts for malectins do not exist in plants, although malectin-like domains (MLDs) are integral constituents of the extracellular region of more than forty membrane-bound receptors in Arabidopsis (Yang et al., 2021). The role of these intrinsic MLDs for receptor function has not yet been fully explored, but it has been suggested that they contribute to the control of plant cell wall integrity (Franck et al., 2018). One of these MLD receptors in Arabidopsis is the leucine-rich repeat receptor-like kinase (MLD-LRR-RLK) IMPAIRED OOMYCETE SUSCEPTIBILITY 1 (IOS1). We previously characterized IOS1 and found it to be a host component that is required for full plant susceptibility to infections with the downy mildew pathogen, *Hyaloperonospora arabidopsidis* (*Hpa*), and other filamentous biotrophic pathogens (Hok et al., 2011, 2014). However, during the interaction between Arabidopsis and the bacterial pathogen *Pseudomonas syringae* the same receptor associates with the pattern recognition receptors (PRRs) FLAGELLIN-SENSITIVE 2 (FLS2) and EF-TU RECEPTOR (EFR), and their co-receptor BRI1-ASSOCIATED RECEPTOR KINASE (BAK1) at the plasma membrane (PM). This interaction seems to stabilize the PRR-BAK1 complexes and enable innate immune signaling upon perception of the corresponding bacterial PATHOGEN-ASSOCIATED MOLECULAR PAT TERNs (PAMPs) (Yeh et al., 2016).

Our studies of the subcellular localization of IOS1 revealed that the receptor is partially retained in the ER. This observation initiated the present study, which ultimately suggests that the diverse activities of IOS1, including its adapted responses toward different invading pathogens, primarily rely on its structural modularity. This unique modularity enables domains to engage cellular responses in distinct subcellular compartments of the plant cells.

## RESULTS

### The malectin-like domain of IOS1 causes receptor retention in the ER

The IOS1 receptor is a ~100 kDa protein with a particular modular domain structure. It is composed of an N-terminal signal peptide for ER-mediated secretion, the MLD, two leucine-rich repeat (LRR) motifs, a single transmembrane-spanning (TM) region, and an intrinsic kinase domain (Figure 1A). The protein is predicted to localize to the PM, with the C-terminal kinase being cytoplasmic and both the MLD and the LRRs being extracellular. To confirm the predicted localization, we performed transient co-expression experiments in *Nicotiana benthamiana* with C-terminal red fluorescent protein (RFP)-tagged IOS1. In these experiments, we found IOS1 co-localizing with the N-terminal CITRINE-tagged tandemly repeated Pleckstrin Homology (PH) domain from phosphoinositide phospholipase C (construct 2xPLC), which binds phosphatidylinositol lipids within the PM (Van Leeuwen et al., 2007), thus confirming PM localization of IOS1 (Figure 1A, left column). However, red fluorescence of the IOS1-RFP fusion also occurred in intracellular structures resembling the endoplasmic reticulum (ER). An analysis of >50 regions of interest on the confocal images according to (Medina-Puche et al., 2021) revealed mean intensity values of 76.2 (±16.6) and 87.1 (±31.4) for the red fluorescence associated with the PM and ER-like structures, respectively. The PM:ER-like ratio of 0.875 thus indicates a nearly equal distribution of the protein between the two compartments. We then performed further transient co-expression experiments with RFP-tagged IOS1 and the construct GFP-HDEL, which generates a fusion between the Wall-Associated Kinase 2 (WAK2) signal peptide and GFP harboring the ER retention signal HDEL at the C-terminus (Nelson et al., 2007). Co-localization between red IOS1 and the green ER marker confirmed that the receptor is partially retained in the ER upon synthesis (Figure 1A, right column).

To analyze whether ER retention involves the MLD, the LRRs, the TM region, or the intracellular kinase, we generated constructs that either harbor the complete extracellular domain followed by the TM region (ED-TM, Figure 1B, left column) or the LRRs, the TM region, and the kinase domain (LRR-TM-kinase, Figure 1B, right column). Both constructs contained the N-terminal IOS1 signal peptide for ER-mediated secretion and C-terminal RFP. These constructs were used in co-localization studies with the ER marker GFP-HDEL. The membrane-anchored ED-TM construct was found to co-localize with the ER marker (Figure 1B, left column). The LRR-TM-Kinase fusion was found in the PM, but did not co-localize with the ER marker protein (Figure 1B, right column). Stably transformed Arabidopsis lines that produced either the

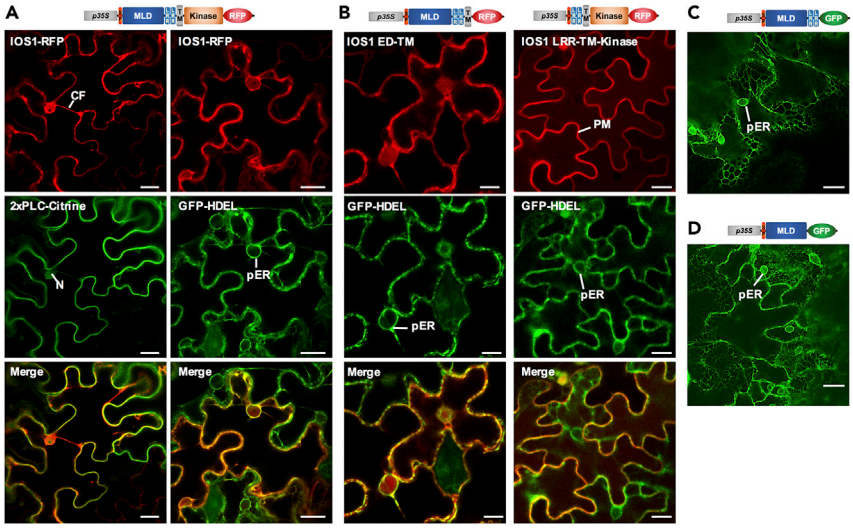


**Figure 1. The MLD retains IOS1 in the ER**

(A) Laser-scanning confocal micrographs showing partial co-localization of RFP-tagged IOS1 with the 2xPLC citrine-tagged PM protein and the GFP-HDEL ER marker upon transient co-expression in *N. benthamiana*. Signals from the Citrine channel were colored in green.

(B) The RFP-labeled IOS1 variant ED-TM with the signal peptide (SP), MLD, LRRs, and membrane-spanning region (TM), but without kinase domain (left panel) co-localizes with green HDEL-GFP, as revealed by yellow-orange color in merged images. The IOS1 variant LRR-TM-Kinase with SP, LRRs, TM, and kinase domain, but without the MLD (right panel) localizes to the PM but does not co-localize with the ER marker.

(C and D) Arabidopsis cotyledons expressing the GFP-fused IOS1 variants consisting of the complete extracellular domain, but devoid of the TM and the kinase domain (C), or of the MLD alone (D). Both variants reside in the ER. Bars represent 10 μM *p35S*, *35S* promoter; CF, cytoplasmic filament; N, nucleus; pER, perinuclear ER.

exodomain of IOS1 (MLD and LRRs, Figure 1C) or the MLD alone (Figure 1D) exhibited strong localization of both GFP-tagged variants to the ER, irrespective of the presence of LRRs (Figures 1C and 1D). Therefore, the MLD appears to be necessary and sufficient for ER localization of the fusion proteins.

We then replaced the constitutive *p35S* promoter with the native *IOS1* promoter (*pIOS1*) and introduced the variant constructs into Arabidopsis marker lines expressing either citrine-labeled Tubby C, a PM-localized transcription factor that translocates to the nucleus (Reitz et al., 2012), or the ER-localized GFP-HDEL protein (Nelson et al., 2007). Subsequently, we analyzed the root elongation zones of the transformant lines, in which the IOS1 promoter is developmentally active (Hok et al., 2014), for the subcellular localization of the different RFP-labeled IOS1 variants (Figure 2). These experiments confirmed our findings from the ones with *N. benthamiana*. They show that native IOS1 co-localizes with both the PM and ER marker (Figure 2A), that IOS1 variants lacking the kinase domain co-localize with the ER marker (Figures 2B–2D), and that a IOS variant lacking the MLD co-localizes with PM-associated Tubby C (Figure 2E, left column), but not with the ER marker (Figure 2E, right column). Taken together, these data indicate that the MLD promotes ER retention of IOS1.

## The MLD of IOS1 attenuates the infection-related UPR and promotes downy mildew disease

The Phyre2 web portal for protein modeling (Kelley et al., 2015) predicts strong structural resemblance between the MLD of IOS1 and the extracellular domain of the Arabidopsis malectin-like receptor kinase ANXUR 1 (Du et al., 2018; Moussu et a., 2018; Figure S1A). The extracellular ANXUR1 domain and the IOS MLD are composed of two subdomains, which both have structural similarities with the ER-residing malectin protein from *Xenopus laevis* (Figures S1B and S1C). Animal malectins contribute to ER stress responses, and because MLD causes ER retention of IOS1, we focused our investigations on a possible role of IOS1-MLD in regulating these responses in the plant cell.

From previous reports, we selected a set of six genes, which are transcriptionally activated during the onset of the two UPR pathways that were described in Arabidopsis (Iwata et al., 2008; Yang et al., 2014); these

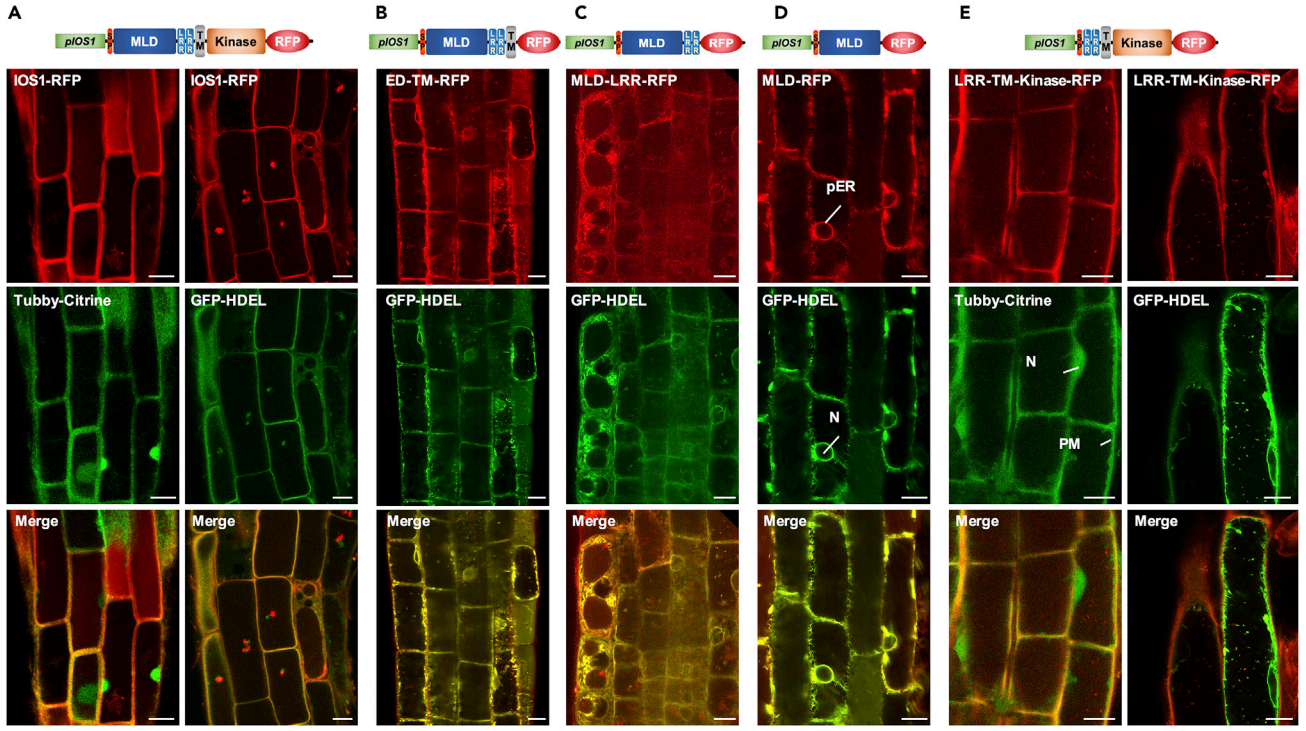


**Figure 2. Localization of IOS1 variants in roots of Arabidopsis marker lines after transgenic expression by the native IOS1 promoter**

Genes encoding the IOS1 variants shown above the micrographs were transformed into Arabidopsis marker lines encoding either the citrine-labeled Tubby-C protein for PM and nuclear localization, or the ER-localized GFP-HDEL protein. Confocal laser-scanning micrographs show the synthesis of the RFP-labeled IOS1 variants in the root cell elongation zone for which developmentally regulated IOS1 promoter activity was previously reported (Hok et al., 2014).

(A) Expression of RFP-tagged native IOS1 in the PM and ER marker lines.

(B) Expression of the RFP-tagged IOS1 variant lacking the kinase domain in the ER marker line.

(C) Expression of the RFP-tagged IOS1 variant lacking the transmembrane (TM) and kinase domains in the ER marker line.

(D) Expression of the RFP-tagged IOS1 variant lacking the LRRs, the TM, and the kinase domain in the ER marker line.

(E) Expression of the RFP-tagged IOS1 variant lacking the MLD in the PM and ER marker lines.

Bars represent 10 μM *pIOS1*, native *IOS1* promoter; N, nucleus; pER, perinuclear ER.

genes code for ADP-RIBOSYLATION FACTOR 1 (ARF1), SECRETION-ASSOCIATED RAS 1 (SAR1), the BINDING PROTEINs one and 3 (BIP1 and BIP3), PROTEIN DISULFIDE ISOMERASE 5 (PDI5), and bZIP60 (Figure S2 and Table S1).

The inoculation of wild-type (wt) Arabidopsis seedlings with *Hpa* stimulates weak transcriptional activation of the abovementioned UPR marker genes. By contrast, *Hpa*-inoculated seedlings from the previously described *ios1-1* mutant (Hok et al., 2011, 2014; Yeh et al., 2016) responded in the same experimental onset with significantly intensified transcriptional activation of all UPR-related genes that were analyzed, when compared to the wt and to the water-treated mutant (Figure 3A). The *ios1-1* mutant also accumulated the spliced version of bZIP60 mRNA upon infection (Figure 3B), which is indicative for activation of the IRE1-mediated UPR (Figure S2) (Nagashima et al., 2011). Taken together, these findings show that the UPR is amplified in the Arabidopsis *ios1-1* mutant upon *Hpa* inoculation, suggesting that IOS1 attenuates this ER stress response in the host when plants are infected with downy mildew.

The increased UPR and decreased susceptibility of *ios1-1* plants suggest a relationship between the intensity of ER stress responses and the outcome of downy mildew disease. To analyze the potential correlation between the two phenotypes, we employed a pharmacological approach. We treated Arabidopsis seedlings with dithiothreitol (DTT) and tunicamycin (Tm), drugs that stimulate the UPR in plants (Martinez and Chrispeels, 2003), and with 4-phenylbutyric acid (4-PBA), a drug that has been shown to attenuate it (Watanabe and Lam, 2008). We then inoculated the treated seedlings with *Hpa* and analyzed spore formation at the end of the infection cycle as an indicator of disease susceptibility (Hok et al., 2011, 2014). Compared to control seedlings, *Hpa* proliferation was significantly increased in 4-PBA-treated plants, but reduced in

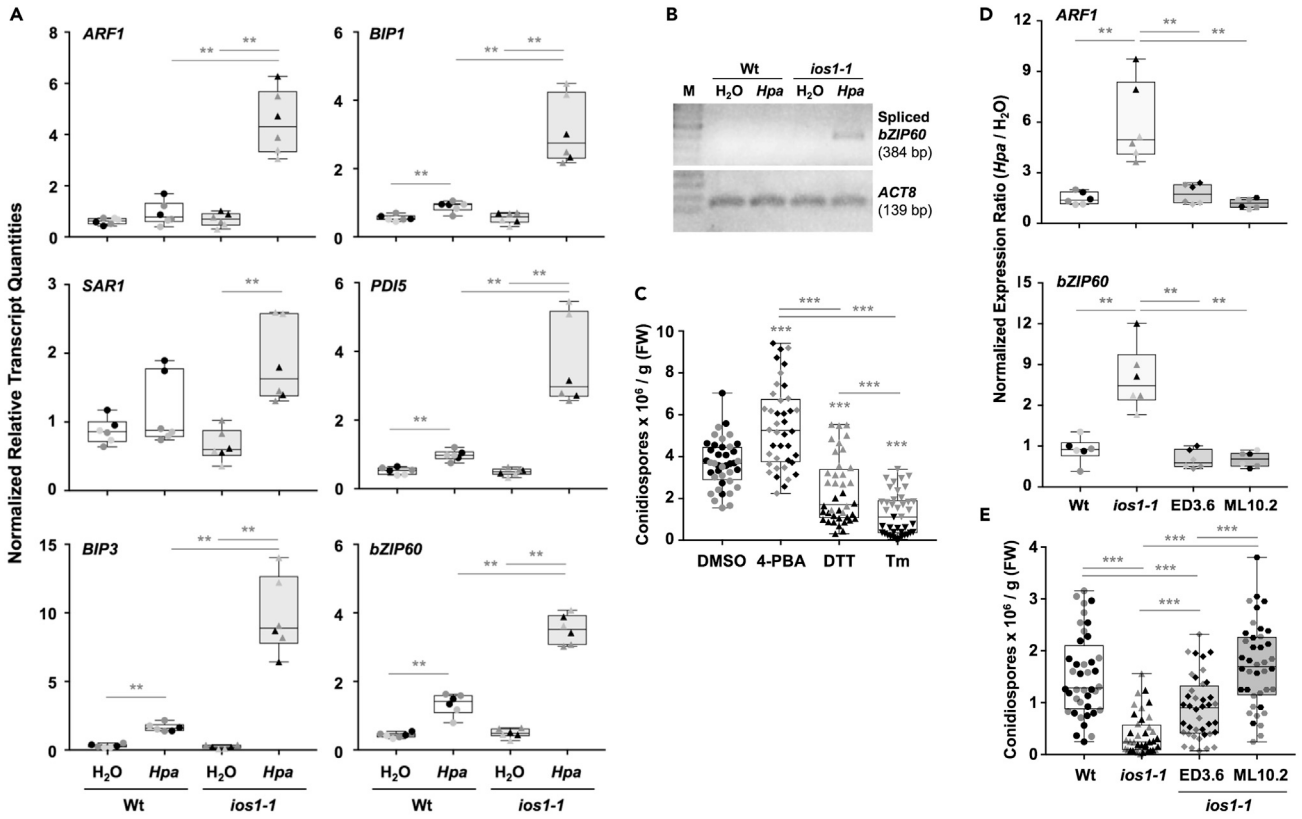


**Figure 3. The IOS1 MLD attenuates pathogen-induced ER stress and promotes susceptibility to *Hpa***

(A) The accumulation of *UPR* gene transcripts is increased in *Hpa*-infected *ios1-1* mutant seedlings when compared to the wild-type (wt), as analyzed by RT-qPCR. Samples were collected 4 days after control treatment ($H_2O$) or infection (*Hpa*).

(B) *Hpa*-inoculated *ios1-1* mutants produce spliced *bZIP60* mRNA. RT-PCR was performed with selective primers on transcripts extracted from $H_2O$-treated and *Hpa*-infected wt and *ios1-1* mutant plantlets. M, 100 bp DNA ladder.

(C) Chemical inhibition and induction of the UPR promotes and represses plant susceptibility to *Hpa*, respectively. Seedlings were treated with DMSO (Control), 4-PBA, DTT, or Tunicamycin (Tm).

(D) Enhanced ER stress in *ios1-1* upon *Hpa* inoculation is attenuated to wt levels by the MLD. Accumulation of *ARF1* and *bZIP60* gene transcripts was analyzed by RT-qPCR in wt and *ios1-1* mutant seedlings, and in those from the complemented mutant lines ED3.6 and ML10.2, and expressed as the ratio between inoculated and uninoculated plants.

(E) The MLD restores susceptibility in the *ios1-1* mutant.

RT-qPCR data in (A) and (D) are from three biological replicates each involving two technical replicates. Data were analyzed using *ACT8* and *UBQ10* as reference genes. Sporulation rates in (C) and (E) were determined seven dpi as a parameter for disease susceptibility. Shown are the amounts of conidiospores per g fresh weight (FW) from two biological replicates each consisting of 20 samples. Statistically significant differences for RT-qPCR data and sporulation assays were determined by the nonparametric Mann-Whitney test and the paired t test, respectively. Significance groups are represented by stars above the boxplots in the respective graphs (*, $p < 0.05$; **, $p < 0.01$; ***, $p < 0.001$). Biological replicates are represented in all Box Whisker plots by different gray tones.

See also Figures S1, S2, S3, and S4.

seedlings treated with DTT or Tm (Figure 3C). These results indicate that the UPR in the host plant negatively influences infection by *Hpa*.

To analyze whether the full-length receptor is required for attenuating ER stress, or whether individual IOS1 domains are sufficient, we generated *ios1-1* mutant lines that express either the complete extracellular domain with the membrane-spanning region (line ED3.6), or the MLD alone (line ML10.2), both with the N-terminal IOS1 signal peptide for ER-mediated secretion. We inoculated seedlings from these lines with *Hpa* and compared the accumulation of transcripts from the UPR marker genes *ARF1* and *bZIP60* with the accumulation of mRNA occurring in uninoculated plants from the same lines (Figure 3D). In both lines, the amplified pathogen-induced expression of UPR-related genes conferred by the *ios1-1* mutation was attenuated to near-Wt levels, thus complementing the ER stress response phenotype of

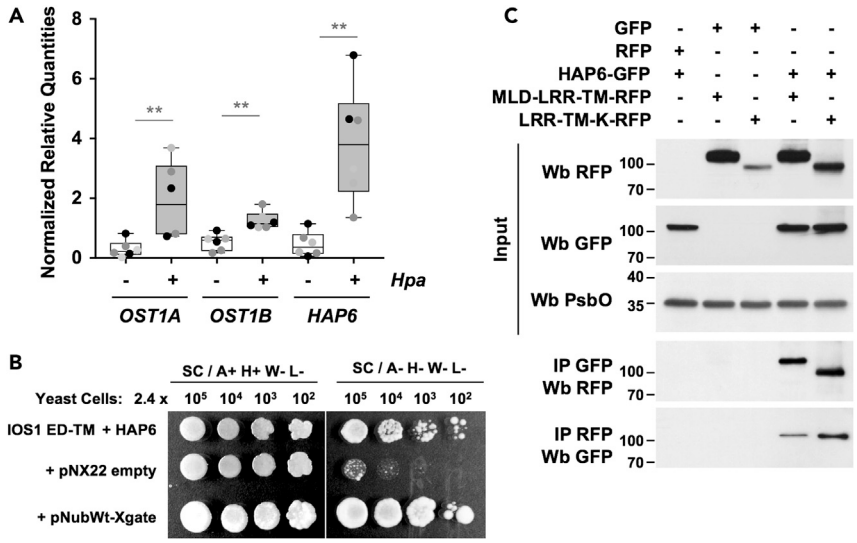


**Figure 4. The IOS1 exodomain associates with the ribophorin HAP6 in the ER**

(A) *OST1A*, *OST1B*, and *HAP6* transcript accumulations upon infection of wt plants with *Hpa*, as quantified by RT-qPCR using expression of the Actin8-encoding gene as internal standard for normalization. RT-qPCR data are from three biological replicates, each involving two technical replicates. Data were analyzed using *ACT8* and *UBQ10* as reference genes. Asterisks indicate statistically significant differences as determined by nonparametric Mann-Whitney tests (**, $p < 0.01$). Biological replicates are represented by dots in different gray tones.

(B) Co-expression of the extracellular IOS1 domain (ED-TM) bait with the HAP6 prey in the mb-SUS Y2H system allows cells to grow on synthetic complete (SC) medium in the absence of adenine (A) and histidine (H), indicative for physical association between the proteins. Growth on SC medium containing A and H, but neither tryptophan (W) nor leucine (L) confirmed accomplished mating. The empty pNX32 prey vector shows absence of autoactivation by the ED-TM bait. The pNubWt-Xgate vector positively controls yeast growth.

(C) Co-immunoprecipitation of IOS1 domains with HAP6 upon transient expression in *N. benthamiana*. Production of the RFP-labeled IOS1 variants and GFP-labeled HAP6 in protein preparations was controlled on Western blots (Wb; Input, top panels). Precipitated proteins with anti-GFP and anti-RFP beads were revealed by Wb with anti-RFP and anti-GFP antibodies, respectively (IP, bottom panels). An antibody against the plant photosystem II PsbO protein was used for Input normalization. Please note that the apparent molecular mass of the MLD-LRR-TM-RFP variant is higher than the expected one (84 kDa) because of N-glycosylations of the IOS1 exodomain.

See also Figures S5, S6, and S7.

the *ios1-1* mutant (Figure 3D). These findings indicate that the IOS1 MLD is sufficient to attenuate the UPR in the host during the interaction with downy mildew. The same lines were then inoculated and analyzed for *Hpa* sporulation levels. We found that the reduced susceptibility phenotype of the *ios1-1* mutant was restored to near wt levels when the MLD-containing IOS1 variants were expressed in the *ios1-1* background (Figure 2E). These data and observations taken together suggest that the MLD of IOS1 attenuates pathogen-induced ER stress responses, thus favoring infection with downy mildew.

It should be noted that a second allelic mutant line, *ios1-2*, did not exhibit the phenotype of reduced susceptibility to *Hpa* infection characteristic of *ios1-1* (Figure S3A) (Hok et al., 2014). The *ios1-2* mutants were also not altered in their pathogen-induced ER stress responses, when compared to the Wt. Significant differences in pathogen-induced expression of the UPR marker genes ARF1 and bZIP60 between wt and *ios1-2* mutant plants were not detectable (Figure S3B). The *ios1-1* insertional mutation resides in the MLD-encoding sequence of the *IOS1* gene, whereas the *ios1-2* insertion is located in the first quarter of the kinase domain (Figure S4). It has been previously shown that the mutant IOS1-2 allele is transcribed to the insertion site in mRNA that comprises the coding region for a IOS1 variant with a truncated kinase domain (Hok et al., 2014; Yeh et al., 2016).

## IOS1 associates with the ribophorin HAP6 in the ER

When wt plants were either treated with water or inoculated with the downy mildew pathogen, the accumulation of transcripts from the three ribophorin-encoding genes in Arabidopsis was induced in

*Hpa*-infected plants, when compared to the water-treated controls. However, transcripts from the HAP6 gene accumulated most abundantly (Figure 4A). The gene encoding HAP6 was previously shown to limit the infection success of a filamentous biotroph on Arabidopsis, as *rpn2/hap6* knockdown mutant lines better support development of the powdery mildew pathogen, *Erysiphe cruciferarum* (Weis et al., 2013). Given this phenotype and the transcript accumulation we observed upon *Hpa* infection, we hypothesized that RPN2/HAP6 might be an ER-localized interacting partner for the exodomain of IOS1.

To investigate a potential association between the membrane-anchored exodomain of IOS1 and HAP6, we first used the mating-based split-ubiquitin yeast two-hybrid system (mbSUS), which has been developed to detect interactions between membrane-bound proteins and their partners (Grefen et al., 2009). Detection is possible when physical proximity of two ubiquitin halves on the cytoplasmic side of the membrane triggers the proteolytic release of a transcriptional activator and its translocation to the nucleus. HAP6 is anchored with three transmembrane domains at the outermost C terminus in the ER membrane, whereas the main part of the protein with the N-terminus resides in the ER lumen (Jeong et al., 2018; Tsirigos et al., 2015; Figure S5). We thus developed transcriptional fusion constructs that generate both the ED-TM bait and the HAP6 prey with an ubiquitin half at the cytoplasmic C-terminus. Mated yeast transformants expressing the ED-TM bait with the HAP6 prey readily grew on selective medium, suggesting physical proximity between the two proteins (Figure 4B). We then tested whether both proteins localize to the same subcellular compartments in plant cells. We generated a *HAP6* gene construct with a C-terminal GFP tag and used it for transient co-expression experiments in *N. benthamiana* with the abovementioned ED-TM-RFP construct. Confocal imaging showed that the expressed HAP6-GFP and ED-TM-RFP proteins display similar localization pattern and merged images of cells that express both proteins reveal their co-localization in perinuclear and peripheral cell structures that apparently represent the ER (Figure S6). To confirm these findings; we used two RFP-tagged IOS1 variant constructs lacking either the kinase (MLD-LRR-TM-RFP) or the MLD (LRR-TM-K-RFP), and GFP-tagged HAP6 (HAP6-GFP) for transient Agrobacterium-mediated co-expression in *N. benthamiana*. Western blots (Wb) with protein extracts from the transfected leaf tissues and antibodies directed against RFP and GFP revealed the presence of the expressed proteins (Figure 3C, Input). The fractions were then submitted to co-immunoprecipitation (Co-IP) with GFP-traps and RFP-traps, and analyzed for the presence of RFP-tagged proteins upon GFP trapping and *vice versa*. These experiments showed that both IOS1 variants pull down HAP6 and that HAP6 pulls-down both variants, suggesting that the receptor variants and the ribophorin form part of the same complex (Figure 4C). Because HAP6 lacks a cytoplasmic domain, it is unlikely that complex formation involves the cytoplasmic IOS1 kinase. It seems more likely that the LRR motifs of IOS1 in the ER lumen and/or the TM domain and some juxtaposed amino acids are involved, as these regions are the only common elements of the two IOS1 variants that interact with HAP6 in co-IP experiments.

## HAP6 promotes ER stress and attenuates susceptibility to *Hpa*

The Arabidopsis *hapless* full knockout mutant *hap6* has disrupted male functions and the corresponding mutation can only be maintained in plants that are heterozygous for the locus (Johnson et al., 2004). We obtained two other allelic T-DNA insertion lines for *HAP6* that are homozygous for the mutation, and which previously had been designated as *rpn2-1* and *rpn2-2* (Weis et al., 2013). However, the T-DNA insertions in these lines reside in the 15$^{th}$ intron (*rpn2-1*) and in the 5′UTR (*rpn2-2*), and both lines still produce *HAP6* transcripts although to a lesser extent than the wt (Figure S8) (Weis et al., 2013). To analyze whether HAP6 contributes to the plant responses to downy mildew, we inoculated wt and *hap6* mutant seedlings with *Hpa* and analyzed the expression of marker genes for ER stress responses. Infection of seedlings from the wt induced a slight but significant increase in the accumulation of *ARF1* and *bZIP60* transcripts (Figure 5A). This pathogen-induced ER stress response was not observed in seedlings from the two allelic *hap6* knockdown lines, suggesting that HAP6 contributes to activation of the UPR upon downy mildew infection. We analyzed the sporulation of *Hpa* on infected seedlings from the wt and the *hap6* mutant lines, and noticed a weak but significant increase of sporulation on mutant seedlings when compared to the wt (Figure 5B). A similar slightly enhanced sporulation rate was previously observed upon infection of these *hap6* mutants with the fungal powdery mildew pathogen (Weis et al., 2013). To further investigate the interaction phenotype, we quantified the expression of the *Hpa* gene *Ppat5* (Bittner-Eddy et al., 2003) at a time point of invasive growth of the oomycete in plant tissues. We found significantly more abundant *Ppat5* transcript accumulation in the *hap6* mutants when compared to the wt (Figure 5C), suggesting that the pathogen more effectively invades plant tissues with downregulated *HAP6* expression. Taken together, these

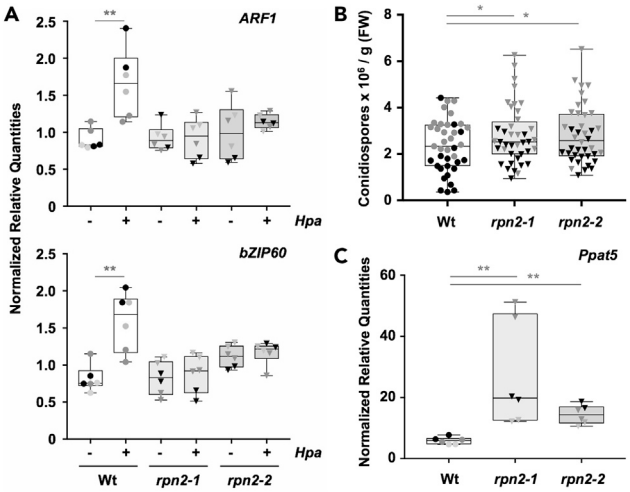


**Figure 5. HAP6 promotes ER stress and attenuates susceptibility to *Hpa***

(A) Expression of *ARF1* and *bZIP60* in wt and the allelic *rpn2-1* and *rpn2-2* knock-down mutants, 4 days after water treatment (-) or inoculation with *Hpa* (+).

(B) *Hpa* sporulation on wt, *rpn2-1*, and *rpn2-2* seedlings, as determined 7 days after inoculation. Shown are the amounts of conidiospores per g fresh weight (FW) from two biological replicates, each consisting of 20 samples.

(C) Accumulation of transcripts from the downy mildew *Ppat5* gene, 4 days after inoculation of wt, *rpn2-1*, and *rpn2-2* seedlings.RT-qPCR data in (A) and (C) were analyzed using *ACT8* and *UBQ10* as reference genes and are from three biological replicates each consisting of two technical replicates.

Statistically significant differences for RT-qPCR data and sporulation assays were determined by the nonparametric Mann-Whitney test and the paired t test, respectively. Significance groups are represented by stars above the boxplots in the respective graphs (*, $p < 0.05$; **, $p < 0.01$; ***, $p < 0.001$). Biological replicates are represented in all Box Whisker plots by different gray tones.

See also Figures S2 and S8.

findings indicate that HAP6, along with the extracellular domain of IOS1, contributes to the regulation of ER stress responses during the infection of plant tissues with downy mildew.

## DISCUSSION

The results presented here may reconcile previous debates about the role of IOS1 in the interaction of Arabidopsis with pathogens. On the one hand, IOS1 promotes plant susceptibility to infection by filamentous biotrophic or hemibiotrophic pathogens (Hok et al., 2011, 2014). On the other hand, it contributes to immune responses to the bacterium *P. syringae* by its association with PRRs and the co-receptor BAK1 (Yeh et al., 2016). Here, we show that IOS1 attenuates downy mildew-induced ER stress signaling. The *ios1-1* mutant phenotypes, i.e., upregulated UPR upon infection and reduced disease susceptibility to *Hpa*, are countervailed by expression of MLD-containing IOS1 variants in the mutant background. The kinase domain appears not to be involved in the here-described IOS1 activities in the ER. By contrast, this domain seems to be important for stabilizing PRR receptor complexes at the PM. The kinase domains of FLS2 and EFR pull down the IOS1 kinase in *in vitro* assays, and the association between FLS2 and BAK1 is impaired in the *ios1-2* insertion mutant, which is supposed to produce a IOS1 variant with a truncated kinase (Yeh et al., 2016; compare Figure S4). Taken together, the data suggest that individual domains of the same receptor may have divergent activities in different subcellular compartments. Although the MLD of IOS1 reduces pathogen-induced stress responses in the ER and increases the infectivity of *Hpa*, the kinase domain of the receptor promotes immune signaling at the PM, leading to increased resistance to the bacterium (Figure 6). This interpretation might also explain different findings for allelic *ios1* mutant phenotypes. Only *ios1-1* with an insertion in the MLD-encoding sequence presents phenotypes involving *Hpa*, but not the allelic *ios1-2* and *ios1-3* insertion mutants, which are interrupted in the kinase domain (Hok et al., 2014; Figures S3 and S4).

The sequence and predicted structure of the extracellular MLD of IOS1 are similar to the MLDs of other Arabidopsis receptor kinases such as FERONIA (FER) and ANXUR (ANX1 and ANX2; see Figure S1). FER

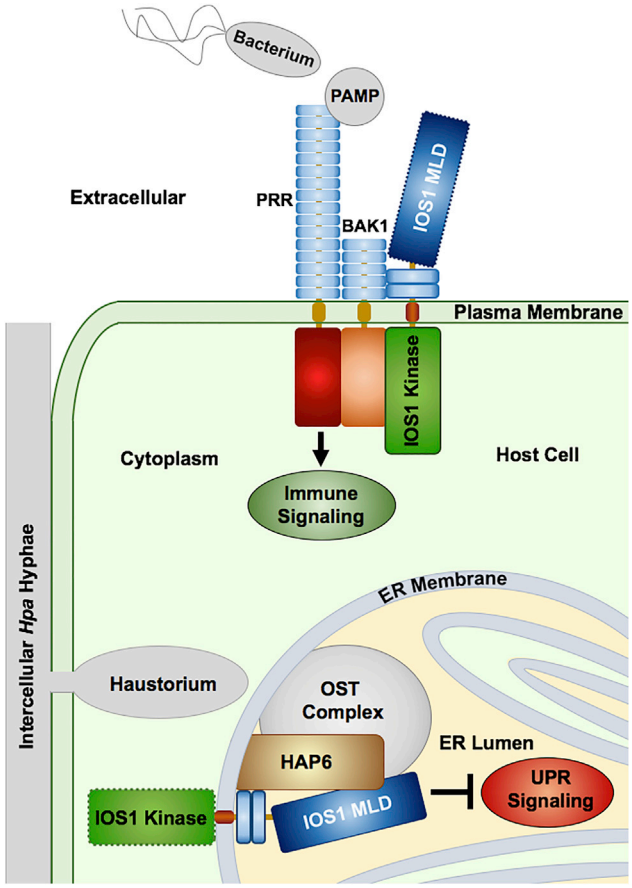


**Figure 6. Proposed roles for individual domains of the IOS1 receptor during the interaction with bacteria and filamentous biotrophs**

As previously reported (Yeh et al., 2016) IOS1 stabilizes the complex between the pattern-recognition receptors (PRR) FLS2 and EFR with their co-receptor BAK1 at the PM. Stabilization involves the IOS1 kinase domain and fortifies pathogen-associated molecular pattern (PAMP)-triggered immune responses. Knockout mutants for the IOS1 kinase are thus more susceptible to bacterial infection. Filamentous biotrophic fungi and oomycetes establish feeding sites called haustoria inside living host cells. Subsequent increased metabolic activity and protein synthesis in the host cell generates ER stress and triggers the unfolded protein response (UPR). The UPR is positively regulated by the ribophorin HAP6 and probably other compounds of the Oligosaccharyltransferase (OST) complex. The infection stimulates synthesis of IOS1 that transits to the ER, where the MLD disables the infection-related UPR, and promotes the development of the pathogen. The knockout mutant for the IOS1 MLD is thus less susceptible to infection by filamentous biotrophs. Receptor domains with dotted outlines appear dispensable for the indicated functions at the PM or the ER.

and ANX have multiple functions during development, reproduction, and perception of environmental stimuli and were originally identified as important regulators of fertility in Arabidopsis (Escobar-Restrepo et al., 2007; Boisson-Dernier et al., 2009; Miyazaki et al., 2009). Similar to IOS1, FER and ANX serve as scaffolds for complex formation of Arabidopsis PRRs with BAK1, but affect immune signaling against *P. syringae* antagonistically despite the close homology of their MLDs. Although FER promotes immunity against the bacterium (Stegmann et al., 2017), ANX attenuates it (Mang et al., 2017). Mutations in the FER gene make plants more susceptible to bacterial infection, similar to what is observed in *ios1* mutants. But like the *ios1-1* mutant (Hok et al., 2014), *fer* mutants were also less susceptible to infection by the filamentous biotrophic powdery mildew pathogen (Kessler et al., 2010). These observations suggest that FER, ANX, and IOS1 fine-tune the interaction of Arabidopsis with the biotic environment with additional receptor functions distinct from those contributing to the scaffold of PRR complexes. ER retention has not yet been observed for FER and ANX, but FER was shown to establish in the ER a complex with the glycosylphosphatidylinositol-anchored protein (GPI-AP) Lorelei-like GPI-AP1 (LLG1). LLG1 acts as a chaperone for the receptor, and guides FER to the PM where LLG1 functions as a co-receptor for the Rapid

Alkalinization Factor (RALF) peptide ligand of FER (Li et al., 2015; Xiao et al., 2019). The absence of LLG1 in a mutant leads to ER retention of FER (Li et al., 2015).

ER stress responses and the UPR are closely linked to other regulatory mechanisms for cellular homeostasis (such as autophagy) and ultimately determine cell death or cell survival (Srivastava et al., 2018). Therefore, it is not surprising that pathogens, which manipulate the metabolism of the plant and require living host cells for feeding (at least during a period of their life cycle), seek to repress ER stress responses (Jing et al., 2016; Fan et al., 2018). Haustoria of invading filamentous biotrophs are surrounded by the host ER and Golgi bodies, which supply lipids and proteins for PM expansion and cellular remodeling (Koh et al., 2005). It is likely that this exploitation of plant organelles and their overstraining lead to ER stress responses that impair pathogen development. Infection of Arabidopsis with downy mildew leads to stimulation of the UPR (Figure 3) and to transcriptional activation of IOS1 synthesis in plant cells harboring haustoria (Hok et al., 2014). The nascent receptor can be retained in the ER, where it interacts with the ER membrane-associated ribophorin HAP6. HAP6 functions during plant-microbe interactions are not yet well characterized. It is an essential compound of the OST complex, which catalyzes asparagine (N)-linked glycosylation of nascent proteins and ensures correct protein folding in the ER (Jeong et al., 2018). This process is part of the cellular ER quality control, which also supports the appropriate folding and modification of plant immune receptors (Eichmann and Schäfer, 2012). We also observed that the IOS1 exodomain becomes N-glycosylated during receptor synthesis (Figure S7). The observed association of HAP6 with IOS1, likely involving the LRRs of IOS1, may reflect the stage at which the OST complex takes over the receptor for N-glycosylation. Based on the present results, we propose a simplified scenario, in which HAP6 promotes the UPR in Arabidopsis upon downy mildew infection. The infection also stimulates IOS1 synthesis, binding of the nascent protein to HAP6 in the ER, and attenuation of the UPR-promoting activity of HAP6 by the MLD. This provides the downy mildew pathogen with an advantage for establishing disease (Figure 6).

It has been shown previously that HAP6 also establishes physical interaction with the ER-resident BAX INHIBITOR-1 (BI-1) protein in Arabidopsis (Weis et al., 2013). BI-1 is required for full plant susceptibility to biotrophic filamentous pathogens such as the powdery mildew fungus (Eichmann et al., 2010), and plays a pivotal role as a survival factor against ER stress-mediated programmed cell death (Watanabe and Lam, 2008). However, the molecular mode of action of BI-1 in the ER of plant cells is not yet clear. In animal cells, BI-1 forms a stable protein complex with IRE1α and decreases the IRE1 ribonuclease activity. This prevents bZIP60 mRNA splicing and suppresses the UPR (Lisbona et al., 2009). It was also shown that BI-1 suppresses autophagy in animal cells, and the authors suggested that this effect is a consequence of inhibition of the UPR by the BI-1/IRE1α complex. The cell death-suppressing effect of BI-1 would then eventually be determined by interference with autophagy, which results from the BI-1/IRE1α interaction and inhibition of the UPR (Castillo et al., 2011). At present, no experimental support for physical interaction between BI-1 and IRE1 in plant cells is available, and it has even been considered that IRE1 and BI-1 orchestrate two independent ER stress response pathways in plants (Gaguancela et al., 2016). All findings from our studies and previous reports taken together (i.e., complex formation between BI-1 and HAP6 (Weis et al., 2013); interaction of HAP6 with IOS1 (this report); antagonism of the proteins on the IRE1/bZIP60-mediated UPR upon infection with downy mildew (this report)), we suggest a hypothetical mechanistic scenario for the observed UPR regulation during the interaction with the downy mildew pathogen. BI-1 inhibits the UPR by interacting with IRE1 subunits, thereby eventually repressing cell death. HAP6 stimulates the UPR by binding and displacing the UPR-repressor BI-1. Infection with downy mildew in turn stimulates production of IOS1, which displaces HAP6 from BI-1. BI-1 would then be available again for repressing the UPR and cell death, thus promoting *Hpa* to complete its life cycle in living plant tissues

Our study provides answers to some of the many questions about the role of IOS1. More generally, it suggests that modular plant receptors can extend their activities through the complex topology of different domains that can act independently of the other regions of the protein.

## Limitations of the study

In this study, we show that the MLD of IOS1 retains the receptor in the ER and that it is sufficient to complement the *Hpa*-related phenotypes of the *ios1-1* mutant, i.e., increased UPR upon infection and reduced susceptibility to the downy mildew pathogen. IOS1 forms a complex with HAP6, a protein that affects the UPR and plant susceptibility in a manner opposite to that of IOS1. This observation suggested that the MLD retains IOS1 in the ER and suppresses the UPR through physical interaction with HAP6. However, co-IP data

show that a IOS1 variant lacking the MLD (LRR-TM-kinase variant) can associate with HAP6, but this variant localizes to the PM and not the ER. In addition, the MLD alone can complement *ios1-1* phenotypes, whereas complex formation between IOS1 and HAP6 appears to require a protein environment containing the LRRs (and/or TM domain) and not necessarily the MLD. These data rather indicate that physical interaction with HAP6 alone is not responsible for either ER retention of IOS1 or suppression of the UPR by the MLD. Therefore, we suggest that IOS1 forms higher-order complexes in the ER with as yet unknown proteins in addition to HAP6. Such complex partners could be other components of the OST complex (such as OST1A and OST1B) or components of the IRE1/bZIP28-regulated UPR signaling pathways. Moreover, the role of the kinase domain in the function of IOS1 remains ambiguous, and the possibility that this domain also exerts additional functions in the regulation of ER stress cannot be ruled out. The study presented here should therefore be considered as a starting point for further elucidation of the mechanisms that allow IOS1 domains to regulate the UPR in the ER of plant cells.

## STAR★METHODS

Detailed methods are provided in the online version of this paper and include the following:

- KEY RESOURCES TABLE
- RESOURCE AVAILABILITY
  - Lead contact
  - Materials availability
  - Data and code availability
- EXPERIMENTAL MODEL AND SUBJECT DETAILS
  - Arabidopsis thaliana
  - Nicotiana benthamiana
  - Hyaloperonospora arabidopsidis
- METHOD DETAILS
  - Gene constructs
  - Transformation
  - Plant treatments
  - PCR
  - Yeast two-hybrid
  - Proteins
  - Immunological methods
  - Live cell imaging
- QUANTIFICATION AND STATISTICAL ANALYSIS

## SUPPLEMENTAL INFORMATION

Supplemental information can be found online at https://doi.org/10.1016/j.isci.2022.103877.

## ACKNOWLEDGMENTS

We thank Dr. Isabelle Fobis-Loisy (ENS, Lyon, France) for the 2xPLC-CIT construct and the Tubby-C Arabidopsis line. We thank the late Professor Chris Hawes (Oxford Brookes University, UK) for the GFP-HDEL marker line. We are grateful to Dr. Michael Quentin, Dr. Joffrey Mejias, and Dr. Maëlle Jaouannet for helpful discussions. We thank Dr Aurélien Boisson-Dernier for proofreading the manuscript and Dr. Abby Cuttriss for editing the English. We gratefully acknowledge the tools provided on smart.servier.com that helped us design the graphical abstract. This work was supported by the French Government (National Research Agency, ANR) through the "Investments for the Future" LABEX SIGNALIFE: program reference # ANR-11-LABX-0028-01, and by the INRAE SPE department.

## AUTHOR CONTRIBUTIONS

L.G., F.P., B.B.-M., and H.K. designed the study and experiments. L.G. and H.K. wrote the manuscript. L.G. performed yeast two-hybrid analysis and pull-down experiments. L.G., V.A., A.C., and S.H. performed all other experiments.

## DECLARATION OF INTERESTS

The authors declare no competing interests.

Received: October 14, 2019
Revised: January 6, 2022
Accepted: February 2, 2022
Published: March 18, 2022

## SUPPORTING CITATIONS

The following reference appears in the Supplemental information: Pettersen et al., 2004.

## REFERENCES

Angelos, E., Ruberti, C., Kim, S.J., and Brandizzi, F. (2017). Maintaining the factory: the roles of the unfolded protein response in cellular homeostasis in plants. Plant J. *90*, 671–682.

Bittner-Eddy, P.D., Allen, R.L., Rehmany, A.P., Birch, P., and Beynon, J.L. (2003). Use of suppression subtractive hybridization to identify downy mildew genes expressed during infection of *Arabidopsis thaliana*. Mol. Plant Pathol. *4*, 501–507.

Boisson-Dernier, A., Roy, S., Kritsas, K., Grobei, M.A., Jaciubek, M., Schroeder, J.I., and Grossniklaus, U. (2009). Disruption of the pollen-expressed FERONIA homologs ANXUR1 and ANXUR2 triggers pollen tube discharge. Development *136*, 3279–3288.

Carvalho, H.H., Silva, P.A., Mendes, G.C., Brustolini, O.J., Pimenta, M.R., Gouveia, B.C., Valente, M.A., Ramos, H.J., Soares Ramos, J.R., and Fontes, E.P. (2014). The endoplasmic reticulum binding protein BiP displays dual function in modulating cell death events. Plant Physiol. *164*, 654–670.

Castillo, K., Rojas-Rivera, D., Lisbona, F., Caballero, B., Nassif, M., Court, F.A., Schuck, S., Ibar, C., Walter, P., Sierralta, J., et al. (2011). BAX inhibitor-1 regulates autophagy by controlling the IRE1α branch of the unfolded protein response. EMBO. J. *30*, 4465–4478.

Chakraborty, R., Uddin, S., Macoy, D.M., Park, S.O., Van Anh, D.T., Ryu, G.R., Kim, Y.H., Lee, J.Y., Cha, J.Y., Kim, W.Y., et al. (2020). Inositol-requiring enzyme 1 (IRE1) plays for AvrRpt2-triggered immunity and RIN4 cleavage in Arabidopsis under endoplasmic reticulum (ER) stress. Plant Physiol. Biochem. *156*, 105–114.

Chen, Y., Hu, D., Yabe, R., Tateno, H., Qin, S.Y., Matsumoto, N., Hirabayashi, J., and Yamamoto, K. (2011). Role of malectin in Glc(2)Man(9) GlcNAc(2)-dependent quality control of α1-antitrypsin. Mol. Biol. Cell. *22*, 3559–3570.

Clough, S.J., and Bent, A.F. (1998). Floral dip: a simplified method for Agrobacterium-mediated transformation of *Arabidopsis thaliana*. Plant J. *16*, 735–743.

Du, S., Qu, L.J., and Xiao, J. (2018). Crystal structures of the extracellular domains of the CrRLK1L receptor-like kinases ANXUR1 and ANXUR2. Protein Sci. *27*, 886–892.

Eichmann, R., and Schäfer, P. (2012). The endoplasmic reticulum in plant immunity and cell death. Front. Plant Sci. *3*, 200.

Eichmann, R., Bischof, M., Weis, C., Shaw, J., Lacomme, C., Schweizer, P., Duchkov, D., Hensel, G., Kumlehn, J., and Huckelhoven, R. (2010). BAX INHIBITOR-1 is required for full susceptibility of barley to powdery mildew. Mol. Plant Microbe. Interact. *23*, 1217–1227.

Escobar-Restrepo, J.M., Huck, N., Kessler, S., Gagliardini, V., Gheyselinck, J., Yang, W.C., and Grossniklaus, U. (2007). The FERONIA receptor-like kinase mediates male-female interactions during pollen tube reception. Science *317*, 656–660.

Fan, G., Yang, Y., Li, T., Lu, W., Du, Y., Qiang, X., Wen, Q., and Shan, W. (2018). A *Phytophthora capsici* RXLR effector targets and inhibits a plant PPIase to suppress endoplasmic reticulum-mediated immunity. Mol. Plant *11*, 1067–1083.

Franck, C.M., Westermann, J., and Boisson-Dernier, A. (2018). Plant malectin-like receptor kinases: from cell wall integrity to immunity and beyond. Annu. Rev. Plant. Biol. *69*, 301–328.

Gaguancela, O.A., Zúñiga, L.P., Arias, A.V., Halterman, D., Flores, F.J., Johansen, I.E., Wang, A., Yamaji, Y., and Verchot, J. (2016). The IRE1/bZIP60 pathway and Bax Inhibitor 1 suppress systemic accumulation of potyviruses and potexviruses in Arabidopsis and *Nicotiana benthamiana* plants. Mol. Plant. Microbe. Interact. *29*, 750–766.

Galli, C., Bernasconi, R., Soldà, T., Calanca, V., and Molinari, M. (2011). Malectin participates in a backup glycoprotein quality control pathway in the mammalian ER. PLoS One *6*, e16304.

Grefen, C., Obrdlik, P., and Harter, K. (2009). The determination of protein-protein interactions by the mating-based split-ubiquitin system (mbSUS). Methods Mol. Biol. *479*, 217–233.

Hetz, C. (2012). The unfolded protein response: controlling cell fate decisions under ER stress and beyond. Nat. Rev. Mol. Cell Biol. *13*, 89–102.

Hetz, C., Zhang, K., and Kaufman, R.J. (2020). Mechanisms, regulation and functions of the unfolded protein response. Nat. Rev. Mol. Cell Biol. *8*, 421–438.

Hiramatsu, N., Chiang, W.C., Kurt, T.D., Sigurdson, C.J., and Lin, J.H. (2015). Multiple mechanisms of unfolded protein response-induced cell death. Am. J. Pathol. *185*, 1800–1808.

Hok, S., Allasia, V., Andrio, E., Naessens, E., Ribes, E., Panabières, F., Attard, A., Ris, N., Clément, M., Barlet, X., et al. (2014). The receptor kinase IMPAIRED OOMYCETE SUSCEPTIBILITY1 attenuates abscisic acid responses in Arabidopsis. Plant. Physiol. *166*, 1506–1518.

Hok, S., Danchin, E.G., Allasia, V., Panabières, F., Attard, A., and Keller, H. (2011). An Arabidopsis (malectin-like) leucine-rich repeat receptor-like kinase contributes to downy mildew disease. Plant Cell Environ. *34*, 1944–1957.

Iwata, Y., Fedoroff, N.V., and Koizumi, N. (2008). Arabidopsis bZIP60 is a proteolysis-activated transcription factor involved in the endoplasmic reticulum stress response. Plant Cell *20*, 3107–3121.

Jeong, I.S., Lee, S., Bonkhofer, F., Tolley, J., Fukudome, A., Nagashima, Y., May, K., Rips, S., Lee, S.Y., Gallois, P., et al. (2018). Purification and characterization of *Arabidopsis thaliana* oligosaccharyltransferase complexes from the native host: a protein super-expression system for structural studies. Plant J. *94*, 131–145.

Jing, M., Guo, B., Li, H., Yang, B., Wang, H., Kong, G., Zhao, Y., Xu, H., Wang, Y., Ye, W., et al. (2016). A *Phytophthora sojae* effector suppresses endoplasmic reticulum stress-mediated immunity by stabilizing plant binding immunoglobulin proteins. Nat. Commun. *7*, 11685.

Johnson, M.A., von Besser, K., Zhou, Q., Smith, E., Aux, G., Patton, D., Levin, J.Z., and Preuss, D. (2004). Arabidopsis hapless mutations define essential gametophytic functions. Genetics *168*, 971–982.

Kadota, Y., Macho, A.P., and Zipfel, C. (2016). Immunoprecipitation of plasma membrane receptor-like kinases for identification of phosphorylation sites and associated proteins. Methods Mol. Biol. *1363*, 133–144.

Karimi, M., Inzé, D., and Depicker, A. (2002). GATEWAY vectors for Agrobacterium-mediated plant transformation. Trend Plant Sci. *7*, 193–195.

Kelley, L.A., Mezulis, S., Yates, C.M., Wass, M.N., and Sternberg, M.J. (2015). The Phyre2 web portal for protein modeling, prediction and analysis. Nat. Protoc. *10*, 845–858.

Kessler, S.A., Shimosato-Asano, H., Keinath, N.F., Wuest, S.E., Ingram, G., Panstruga, R., and Grossniklaus, U. (2010). Conserved molecular components for pollen tube reception and fungal invasion. Science *330*, 968–971.

Koh, S., André, A., Edwards, H., Ehrhardt, D., and Somerville, S. (2005). *Arabidopsis thaliana* subcellular responses to compatible *Erysiphe cichoracearum* infections. Plant J. *44*, 516–529.

Li, C., Yeh, F.L., Cheung, A.Y., Duan, Q., Kita, D., Liu, M.C., Maman, J., Luu, E.J., Wu, B.W., Gates, L., et al. (2015). Glycosylphosphatidylinositol-anchored proteins as chaperones and co-receptors for FERONIA receptor kinase signaling in Arabidopsis. Elife *4*, e06587.

Lisbona, F., Rojas-Rivera, D., Thielen, P., Zamorano, S., Todd, D., Martinon, F., Glavic, A., Kress, C., Lin, J.H., Walter, P., et al. (2009). BAX inhibitor-1 is a negative regulator of the ER stress sensor IRE1alpha. Mol. Cell *33*, 679–691.

Mang, H., Feng, B., Hu, Z., Boisson-Dernier, A., Franck, C.M., Meng, X., Huang, Y., Zhou, J., Xu, G., Wang, T., et al. (2017). Differential regulation of two-tiered plant immunity and sexual reproduction by ANXUR receptor-like kinases. Plant Cell *29*, 3140–3156.

Martínez, I.M., and Chrispeels, M.J. (2003). Genomic analysis of the unfolded protein response in Arabidopsis shows its connection to important cellular processes. Plant Cell *15*, 561–576.

Medina-Puche, L., Kim, C., Lozano-Duran, R., and Dogra, V. (2021). Protocol for evaluating protein relocalization from the plasma membrane to chloroplasts. STAR Protoc. *2*, 100816.

Mishiba, K., Nagashima, Y., Suzuki, E., Hayashi, N., Ogata, Y., Shimada, Y., and Koizumi, N. (2013). Defects in IRE1 enhance cell death and fail to degrade mRNAs encoding secretory pathway proteins in the Arabidopsis unfolded protein response. Proc. Natl. Acad. Sci. U S A *110*, 5713–5718.

Miyazaki, S., Murata, T., Sakurai-Ozato, N., Kubo, M., Demura, T., Fukuda, H., and Hasebe, M. (2009). ANXUR1 and 2, sister genes to FERONIA/SIRENE, are male factors for coordinated fertilization. Curr. Biol. *19*, 1327–1331.

Moussu, S., Augustin, S., Roman, A.O., Broyart, C., and Santiago, J. (2018). Crystal structures of two tandem malectin-like receptor kinases involved in plant reproduction. Acta. Crystallogr. D Struct. Biol. *74*, 671–680.

Nagashima, Y., Mishiba, K., Suzuki, E., Shimada, Y., Iwata, Y., and Koizumi, N. (2011). Arabidopsis IRE1 catalyses unconventional splicing of bZIP60 mRNA to produce the active transcription factor. Sci. Rep. *1*, 29.

Nawkar, G.M., Lee, E.S., Shelake, R.M., Park, J.H., Ryu, S.W., Kang, C.H., and Lee, S.Y. (2018). Activation of the transducers of unfolded protein response in plants. Front. Plant Sci. *9*, 214.

Nelson, B.K., Cai, X., and Nebenführ, A. (2007). A multicolored set of *in vivo* organelle markers for co-localization studies in Arabidopsis and other plants. Plant J. *51*, 1126–1136.

Pettersen, E.F., Goddard, T.D., Huang, C.C., Couch, G.S., Greenblatt, D.M., Meng, E.C., and Ferrin, T.E. (2004). UCSF chimera - a visualization system for exploratory research and analysis. J. Comput. Chem. *25*, 1605–1612.

Qiang, X., Liu, X., Wang, X., Zheng, Q., Kang, L., Gao, X., Wei, Y., Wu, W., Zhao, H., and Shan, W. (2021). Susceptibility factor RTP1 negatively regulates *Phytophthora parasitica* resistance *via* modulating UPR regulators bZIP60 and bZIP28. Plant Physiol. *186*, 1269–1287.

Qin, S.Y., Hu, D., Matsumoto, K., Takeda, K., Matsumoto, N., Yamaguchi, Y., and Yamamoto, K. (2012). Malectin forms a complex with ribophorin I for enhanced association with misfolded glycoproteins. J. Biol. Chem. *287*, 38080–38089.

Reitz, M.U., Bissue, J.K., Zocher, K., Attard, A., Hückelhoven, R., Becker, K., Imani, J., Eichmann, R., and Schäfer, P. (2012). The subcellular localization of Tubby-like proteins and participation in stress signaling and root colonization by the mutualist *Piriformospora indica*. Plant Physiol. *160*, 349–364.

Schallus, T., Jaeckh, C., Fehér, K., Palma, A.S., Liu, Y., Simpson, J.C., Mackeen, M., Stier, G., Gibson, T.J., Feizi, T., et al. (2008). Malectin: a novel carbohydrate-binding protein of the endoplasmic reticulum and a candidate player in the early steps of protein N-glycosylation. Mol. Biol. Cell *19*, 3404–3414.

Srivastava, R., Li, Z., Russo, G., Tang, J., Bi, R., Muppirala, U., Chudalayandi, S., Severin, A., He, M., Vaitkevicius, S.I., et al. (2018). Response to persistent ER stress in plants: a multiphasic process that transitions cells from prosurvival activities to cell death. Plant Cell *30*, 1220–1242.

Stegmann, M., Monaghan, J., Smakowska-Luzan, E., Rovenich, H., Lehner, A., Holton, N., Belkhadir, Y., and Zipfel, C. (2017). The receptor kinase FER is a RALF-regulated scaffold controlling plant immune signaling. Science *355*, 287–289.

Tsirigos, K.D., Peters, C., Shu, N., Käll, L., and Elofsson, A. (2015). The TOPCONS web server for consensus prediction of membrane protein topology and signal peptides. Nucleic Acids Res. *43*, W401–W407.

Van Leeuwen, W., Vermeer, J.E., Gadella, T.W., Jr., and Munnik, T. (2007). Visualization of phosphatidylinositol 4,5-bisphosphate in the plasma membrane of suspension-cultured tobacco BY-2 cells and whole Arabidopsis seedlings. Plant J. *52*, 1014–1026.

Verchot, J., and Pajerowska-Mukhtar, K.M. (2021). UPR signaling at the nexus of plant viral, bacterial, and fungal defenses. Curr. Opin. Virol. *47*, 9–17.

Watanabe, N., and Lam, E. (2008). BAX inhibitor-1 modulates endoplasmic reticulum stress-mediated programmed cell death in Arabidopsis. J. Biol. Chem. *283*, 3200–3210.

Weis, C., Pfeilmeier, S., Glawischnig, E., Isono, E., Pachl, F., Hahne, H., Kuster, B., Eichmann, R., and Hückelhoven, R. (2013). Co-immunoprecipitation-based identification of putative BAX INHIBITOR-1-interacting proteins involved in cell death regulation and plant-powdery mildew interactions. Mol. Plant Pathol. *14*, 791–802.

Xiao, Y., Stegmann, M., Han, Z., DeFalco, T.A., Parys, K., Xu, L., Belkhadir, Y., Zipfel, C., and Chai, J. (2019). Mechanisms of RALF peptide perception by a heterotypic receptor complex. Nature *572*, 270–274.

Xu, Z., Song, N., Ma, L., and Wu, J. (2019). IRE1-bZIP60 pathway is required for *Nicotiana attenuata* resistance to fungal pathogen *Alternaria alternata*. Front. Plant Sci. *10*, 263.

Yang, H., Wang, D., Guo, L., Pan, H., Yvon, R., Garman, S., Wu, H.M., and Cheung, A.Y. (2021). Malectin/Malectin-like domain-containing proteins: a repertoire of cell surface molecules with broad functional potential. Cell Surf. *7*, 100056.

Yang, Z.T., Lu, S.J., Wang, M.J., Bi, D.L., Sun, L., Zhou, S.F., Song, Z.T., and Liu, J.X. (2014). A plasma membrane-tethered transcription factor, NAC062/ANAC062/NTL6, mediates the unfolded protein response in Arabidopsis. Plant J. *79*, 1033–1043.

Yeh, Y.H., Panzeri, D., Kadota, Y., Huang, Y.C., Huang, P.Y., Tao, C.N., Roux, M., Chien, H.C., Chin, T.C., Chu, P.W., et al. (2016). The Arabidopsis malectin-like/LRR-RLK IOS1 is critical for BAK1-dependent and BAK1-independent pattern-triggered immunity. Plant Cell *28*, 1701–1721.

## STAR★METHODS

### KEY RESOURCES TABLE

| REAGENT or RESOURCE | SOURCE | IDENTIFIER |
|---|---|---|
| Antibodies | | |
| anti-IOS1-MLD | ProteoGenix, Schiltigheim, France | antibody designed for this study |
| anti RFP | Chromotek | Cat# 6G6; RRID: AB_2631395 |
| anti-GFP | Chromotek | Cat# 3H9; RRID:AB_10773374 |
| anti-PsbO | Agrisera | RRID: AB_1031788 |
| Goat anti rabbit HRP-coupled secondary antibody | Sigma-Aldrich | Cat# RABHRP1 |
| Goat anti mouse HRP-coupled secondary antibody | Sigma-Aldrich | Cat# 12-349; RRID: AB_390192 |
| Goat anti rat HRP-coupled secondary antibody | Agrisera | Cat# AS10_1187; RRID: AB_10754172 |
| Bacterial and virus strains | | |
| *Agrobacterium tumefaciens* strain GV3101 | LIPME, Auzeville-Toulouse, France | |
| *Escherichia coli* strain DH10B | Thermo Fisher Scientific | 18290015 |
| Chemicals, peptides, and recombinant proteins | | |
| Polyvinylpolypyrrolidone (PVPP) | Sigma-Aldrich | 77627 |
| Phenylmethylsulfonyl fluoride (PMSF) | Sigma-Aldrich | 52332 |
| IGEPAL CA-630 | Sigma-Aldrich | I8896 |
| Sodium molybdate dihydrate ($Na_2MoO_4 \times 2 H_2O$) | Sigma-Aldrich | 331058 |
| Sodium fluoride (NaF) | Sigma-Aldrich | 67414 |
| Activated sodium orthovanadate ($Na_3VO_4$) | Sigma-Aldrich (Calbiochem) | 5086050004 |
| Dimethyl sulfoxide (DMSO) | Sigma-Aldrich | 276855 |
| Kanamycin | ThermoFisher Scientific | 11815024 |
| L-Methionine sulfoximine | Sigma-Aldrich | M5379 |
| Rifampicin | Euromedex | 1059B |
| Spectinomycin | Duchefa Biochemies | S0188 |
| Gentamicin | Euromedex | EU0410-B |
| Acetosyringone | Sigma-Aldrich | D134406 |
| 4-Phenylbutyric acid (4-PBA) | Sigma-Aldrich | P21005 |
| DL-Dithiothreitol (DTT) | Sigma-Aldrich | 43815 |
| Tunicamycin | Sigma-Aldrich | SML1287 |
| Protease Inhibitor Cocktail | Sigma-Aldrich | P9599 |
| Polyvinylpolypyrrolidone (PVPP) | Sigma-Aldrich | 77627 |
| Critical commercial assays | | |
| SuperScript IV Reverse Transcriptase | ThermoFisher Scientific | 18090010 |
| Brilliant III Ultra-Fast SYBR® Green QPCR Master Mix | Agilent | 600882 |
| PNGaseA | New England Biolabs | P0707S |
| PNGaseF | New England Biolabs | P0704S |
| GFP-Trap Magnetic Agarose beads | Chromotek | gtma |
| RFP-Trap Magnetic Agarose beads | Chromotek | rtma |

(*Continued on next page*)

*Continued*

| REAGENT or RESOURCE | SOURCE | IDENTIFIER |
|---|---|---|
| Experimental models: Organisms/strains | | |
| *Arabidopsis thaliana* Landsberg erecta (Ler) ecotype | NASC, UK | N97814 |
| *Arabidopsis thaliana* Columbia (Col) ecotype | NASC, UK | N70000 |
| *Arabidopsis thaliana* GFP-HDEL marker line | Oxford Brookes University, UK | |
| *Arabidopsis thaliana* Tubby-C marker line | ENS, Lyon, France | |
| *Hyaloperonospora arabidopsidis* isolate Wela | MPIZ, Cologne, Germany | |
| *Hyaloperonospora arabidopsidis* isolates Noco2 | MPIZ, Cologne, Germany | |
| *Saccharomyces cerevisiae* $Mat_a$ strain THY.AP4 | Tübingen University, Germany | |
| *Saccharomyces cerevisiae* $Mat_{alpha}$ strain THY.AP5 | Tübingen University, Germany | |
| *ios1-1* | NASC, UK | N176673 |
| *ios1-2* | NASC, UK | N637388 |
| *rpn2-1* | NASC, UK | N519955 |
| *rpn2-1* | NASC, UK | N517994 |
| Oligonucleotides | | |
| Primers, see Table S1 | This paper | N/A |
| Recombinant DNA | | |
| IOS1 | ABRC, Ohio State University, USA | N1G51800ZEF |
| HAP6 | ABRC, Ohio State University, USA | DKLAT4G21150 |
| Gateway pDONR201 | Invitrogen | pDONR 201 |
| pH2GW7 | Plant Systems Biology, VIB, Belgium | pH2GW7 |
| pB7WG2D | Plant Systems Biology, VIB, Belgium | pB7WG2D |
| pB7FWG2 | Plant Systems Biology, VIB, Belgium | pB7FWG2 |
| pK7WG3 | Plant Systems Biology, VIB, Belgium | pK7WG3 |
| pB7RWG2 | Plant Systems Biology, VIB, Belgium | pB7RWG2 |
| pMetYC-DEST | Tübingen University, Germany | RRID:Addgene_105081 |
| pNX22-DEST | Tübingen University, Germany | RRID:Addgene_ 105085 |
| GFP-HDEL | ABRC, Ohio State University, USA | ER-gk/CD3-955 |
| Software and algorithms | | |
| Prism 7.0 | GraphPad, San Diego, USA | |
| qBase 1.3.5 Excel plugin | Biogazelle, Zwijnaarde, Belgium | |
| Fiji ImageJ plugin | Open source software | https://imagej.net/software/fiji/downloads |
| ZEN Digital Imaging for Light Microscopy | Zeiss | RRID:SCR_013672 |
| Phyre2 | Imperial College, London, UK | http://www.sbg.bio.ic.ac.uk/phyre2/html/page.cgi?id=index |
| Chimera V1.10.2 | UCSF, San Francisco, USA | |

## RESOURCE AVAILABILITY

### Lead contact

Further information and requests for resources and reagents should be directed to and will be fulfilled by the Lead Contact, Harald Keller, (harald.keller@inrae.fr).

### Materials availability

Strains, plasmids, and Arabidopsis lines generated in this study are available from the Lead Contact with a completed Materials Transfer Agreement.

### Data and code availability

Data reported in this paper will be shared by the lead contact upon reasonable request.

This paper does not report original code.

Any additional information required to reanalyze the data reported in this paper is available from the lead contact upon reasonable request.

## EXPERIMENTAL MODEL AND SUBJECT DETAILS

### Arabidopsis thaliana

Arabidopsis Wt ecotypes were Landsberg *erecta* (L*er*) and Columbia (Col), and mutant and transgenic lines were generated in these backrounds. Seeds were sown on a soil/sand mixture, stratified for 3 days at 4°C, and then grown under a 12 h photoperiod in a growth chamber at 20°C. The *ios1-1* (GT_5_22250), *ios1-2* (SALK_137388), *rpn2-1* (SALK_019955), and *rpn2-2* (SALK_017994) mutant lines were obtained from the European Arabidopsis Stock Centre. The subcellular marker lines Tubby-C and GFP-HDEL were gifts from Dr. Isabelle Fobis-Loisy (ENS, Lyon, France) and Prof. Chris Hawes (Oxford Brookes University, UK), respectively.

### Nicotiana benthamiana

Plants were grown in soil at 25 °C under a 16 h light and h dark period.

### Hyaloperonospora arabidopsidis

The *Hpa* isolates Wela and Noco were transferred weekly onto the susceptible accessions L*er* and Col, respectively. For infection, 10-day-old plants were spray-inoculated to saturation with a spore suspension of 40,000 spores $mL^{-1}$. Plants were kept in a growth cabinet at 16°C for 6 days with a 12 h photoperiod. Sporulation was induced by spraying plants with water and keeping them for 24 h under high humidity.

## METHOD DETAILS

### Gene constructs

Primers used for Gateway-compatible cloning are listed and described in Table S1. Plasmid N1G51800ZEF was obtained from the Arabidopsis Biological Resource Center (ABRC) at the Ohio State University and used as template for amplifications to generate all IOS1 variant sequences. All constructs contained the IOS1 signal peptide-encoding region, except the LRR-TM-kinase construct, in which an alternative signal peptide sequence was designed with specific primers that also cover the 5′ region of the LRR encoding sequence of IOS1 (Table S1). The HAP6 coding region was amplified from plasmid DKLAT4G21150, which was obtained from the ABRC. For all sequences, two sets of amplicons were generated with primers that introduced, or did not introduce the Stop codon for C-terminal fusions. The amplicons were recombined in the entry vector pDONR201 (Invitrogen) for further swaps to destination vectors. All gene constructs were verified by sequence analysis (Eurofins Genomics, Ebersberg, Germany). Destination vectors were pH2GW7, pB7WG2D, pB7FWG2, pK7WG3, and pB7RWG2 (Plant Systems Biology, VIB, Ghent, Belgium) (Karimi et al., 2002) for transient and stable expression in *N. benthamiana* and Arabidopsis, respectively, and pMetYC-DEST and pNX22-DEST for Y2H analysis using the mbSUS system (Grefen et al., 2009). The native −1,500 bp IOS1 promoter sequence was amplified from Arabidopsis genomic DNA (Hok et al., 2011) with primers allowing to generate amplicons with HindIII- and SpeI-compatible ends (Table S1). The amplicon was ligated in HindIII- and SpeI-digested pB7RWG2 thus allowing replacement of the p35S promoter by the native pIOS1 promoter upstream the attR1 site. Sequences encoding the IOS1 variants were then recombined from pDONR201 into this modified destination vector. All entry-to-destination swaps were performed via Gateway LR clonase reactions (Thermo Fisher Scientific), according to the instructions of the supplier. All gene constructs were verified by sequence analysis (Eurofins Genomics, Ebersberg, Germany). The plasmid containing the GFP-HDEL construct (ER-gk/CD3-955) was obtained

from the ABRC. The plasmid containing the 2xPLC-CIT construct was a kind gift from Dr. Isabelle Loisy (ENS, Lyon, France).

### Transformation

Arabidopsis plants were transformed using the floral dip method (Clough and Bent, 1998) and selected on MS medium plates (1% agar) containing 50 μg/mL kanamycin. Ten independent primary transformants (T1) harboring the constructs were verified by PCR, and homozygous T3 plants were obtained for further analysis. For transient expression analysis, *A. tumefaciens* strain GV3101 containing the different constructs was grown in LB medium supplemented with 50 μg/mL rifampicin, 20 μg/mL gentamicin and 100 μg/mL spectinomycin until $OD_{600}$ reached 1.0. Cells were pelleted, resuspended in infiltration buffer (10 mM $MgCl_2$, 10 mM 2-[N-morpholino] ethanesulfonic acid [MES], pH 5.6, 200 μM acetosyringone) and adjusted to an appropriate optical density, then left for 3h at room temperature in the dark before infiltration. The abaxial side of leaves from 4-week-old *N. benthamiana* was infiltrated using a syringe without a needle. For confocal imaging and protein extraction, leaf patches were collected 48 h after infiltration.

### Plant treatments

Cotyledons of 7 d-old seedlings were sprayed with 0.1 % DMSO-containing solutions of 4-PBA and DTT at 2 mM, and tunicamycin at 7 μM, or with 0.1% DMSO as the control, 6 h before inoculation with Hpa. A second spray-treatment with the solutions was applied during invasive growth of downy mildew at 4 d after inoculation.

### PCR

All methods for RNA extraction, reverse transcription, RT-qPCR and data analyses have been described according to (Hok et al., 2014), except that synthesis of first strand cDNA was performed with the SuperScript IV Reverse Transcriptase (ThermoFisher Scientific, Illkirch, France), and qPCR was performed with an AriaMx Real-time PCR System (Agilent Technologies, Les Ulis, France). Accumulation of spliced bZIP60 mRNA was analyzed by RT-PCR according to (Yang et al., 2014). All primers used for RT-PCR experiments are listed in Table S1.

### Yeast two-hybrid

The mating-based split ubiquitin system (mbSUS) was employed as described (Grefen et al., 2009). The IOS1 ED-TM construct without Stop codon was integrated as bait into pMetYc-DEST and transferred into the haploid $Mat_a$ Yeast strain THY.AP4. The HAP6 sequence without Stop codon was cloned as prey into pNX22-DEST and transferred into the haploid $Mat_{alpha}$ yeast strain THY.AP5. This strain was also transformed for positive and negative control with the prey plasmids, pNubWt-X-gate and empty pNX22-DEST, respectively. Mating between THY.AP4 and THY.AP5 transformants, and selection of diploids for growth on Synthetic Complete minimum (SC) medium complemented with adenine (A) and histidine (H) was performed according to (Grefen et al., 2009). Autotrophic growth of yeast cells was determined at 30°C on SC medium in the absence of adenine and histidine.

### Proteins

*N. benthamiana* leaf discs leaf discs transiently expressing RFP-tagged IOS1 variants and/or GFP-tagged HAP6 and/or free RFP and GFP were sampled 48 h after transfection with *A. tumefaciens*. All samples were frozen in liquid nitrogen, and total proteins were extracted from 5 g of ground material in the presence of sand, 0.5 g PVPP, and 1 mM PMSF in 5 ml extraction buffer (150 mM Tris-HCl pH 7.5 containing 100 mM NaCl, 1 mM EDTA, 0.5% IGEPAL CA-630, 1 mM DTT, 1mM Na2MoO4 × 2H2O, 1 mM NaF, 1.5 mM activated Na3VO4, and 1× Protease Inhibitor Cocktail), precisely according to (Kadota et al., 2016). Protein concentrations in supernatants from the final 15,000 × g centrifugation were determined with the Expedeon Bradford Ultra protein assay (Expedeon, San Diego, CA, USA). Protein concentrations were adjusted in the different samples, supplement with 1× Laemmli loading buffer, incubated at 70°C for 15 min, and loaded on 10% acrylamide gels for SDS-PAGE. Transgenic Arabidopsis seedlings expressing the IOS1 exodomain were sampled in liquid nitrogen, and total proteins were extracted from ground material in extraction buffer (50 mM Tris-HCl buffer, pH 7.5, containing 100 mM NaCl, 0.5% TritonX-100, and 1× Protease Inhibitor Cocktail P9599 (Sigma-Aldrich, Saint-Quentin Fallavier, France)). After 15 min of incubation on ice with agitation, the extracts were centrifuged for 10 min at 5,000 × g. Recovered supernatants were centrifuged in a TLA-120.1 fixed angle rotor (Beckman Coulter, Villepinte, France) at 120,000 × g for 1 h

at 4°C. Supernatants containing the soluble proteins were transferred to fresh tubes and supplemented with 0.05% Triton-X100. Microsomal pellets were washed once with extraction buffer and resuspended in extraction buffer supplemented with 0.01% SDS. Protein concentrations in the samples were determined with the Expedeon BradfordUltra protein assay (Expedeon, San Diego, CA, USA). Protein concentrations were adjusted in the different samples, supplement with 1× Laemmli loading buffer containing 1% SDS, incubated at 95°C for 10 min and loaded on 10% acrylamide gels for SDS-PAGE. PNGase treatments of microsomal proteins were performed with PNGaseA and PNGaseF (New England Biolabs, Ipswich, MA, USA) according to the instructions of the supplier.

### Immunological methods

To produce the antibody directed against the IOS1 MLD, rabbits were immunized with a mixture of the 3 synthetic peptides IGDEYLIRANFLH-cys, cys-YGIDVFDRVWT, and EIYSVNLLP-cys (Figure S5). The antibody was generated, purified and tested by a private company (ProteoGenix, Schiltigheim, France), and was used in Wb experiments in 1:5,000 dilutions. Antibodies directed against GFP and RFP (references 3H9 and 6G6, respectively, Chromotek, Planegg-Martinsried, Germany) were used in 1:10,000 dilutions.

The anti-PsbO antibody (antibody AS06142-33; Agrisera, Vännäs, Sweden) was used in 1:20,000 dilutions. Horseradish peroxidase (HRP)-coupled secondary antibodies directed against rabbit, mouse or rat IgGs (Sigma-Aldrich) were used in 1:20,000 dilutions.

Proteins were transferred on PVDF membranes with the Biorad Trans-Blot® Turbo™ apparatus (BioRad, Marnes-la-Coquette, France), set to the preprogrammed Mixed Molecular Weight Transfer parameters. Membranes were saturated with 5% milk powder in TBS-T (Tris HCl 25 mM, NaCl 140 mM, KCl 3 mM Tween 0.1%), and exposed to primary and secondary antibodies diluted in TBS-T. HRP activity on the membranes was revealed with the ECL Western Blotting Substrate (Promega). Immunoprecipitations were performed with Chromotek GFP- and RFP-Trap Magnetic Agarose beads (gtma and rtma, respectively; Chromotek), which were conditioned according to the recommended procedures. Input extracts were mixed with the beads and incubated for 1h at 4°C under rotation. Beads were trapped with a magnetic bead separation rack (ThermoFisher Scientific), washed 4 times with 10 mM Tris-HCl, pH 7.5 containing 100 mM NaCl and 1 mM EDTA, resuspended in Laemmli loading buffer, and incubated at 70°C for 15 min. Proteins eluted from the beads were separated by SDS-PAGE and analyzed by immunoblotting.

### Live cell imaging

All microscopic analyses were performed at the PlantBIOs imaging facility of the Institut Sophia Agrobiotech. Fluorescence conferred by GFP-, RFP-, and CITRINE-tagged fusion proteins were detected in optical sections of plant tissues by confocal laser scanning microscopy at the on an inverted Zeiss LSM880 microscope (Carl Zeiss France SAS, Marly-le-Roi, France), equipped with Argon ion and HeNe lasers as excitation sources. For simultaneous imaging of GFP, RFP, and/or CITRINE samples were excited at 488 nm, 561 nm, and 516 nm, respectively. Confocal images were acquired with a C-Apochromat 63×/1.20 W Corr M27 objective and processed using the Zeiss ZEN 2 software package.

## QUANTIFICATION AND STATISTICAL ANALYSIS

All graphs are represented as Box and Whisker Plots. Graph design and statistical analyses were performed using the GraphPad Prism 7 software (GraphPad Prism Software Inc., San Diego, CA, USA). Statistically significant differences for RT-qPCR data and sporulation assays were determined by the nonparametric Mann-Whitney test and the paired t test, respectively. Significance groups are represented by stars above the boxplots in the respective graphs (*, $p<0.05$; **, $p<0.01$; ***, $p<0.001$).